Microsyst Technol (2010) 16:1777–1786
DOI 10.1007/s00542-010-1116-7

TECHNICAL PAPER

Numerical investigation of the structure of a silicon six-wafer micro-combustor under the effect of hydrogen/air ratio

Lin Zhu · Tien-Chien Jen · Ying-Feng Ji · Cheng-Long Yin · Mei Zhu

Received: 14 January 2010 / Accepted: 28 June 2010 / Published online: 8 July 2010

Abstract Research reports indicate that sufficiently high equivalence ratio of the hydrogen/air mixture leads to the upstream burning in the recirculation jacket, possibly damaging the micro- combustor due to the high wall temperature. This work investigates the influences of the equivalence ratio of the mixture on the structure of a micro-combustor device. Numerical simulation approaches focused on the structural design of the micro-combustor with the flame burning in the recirculation jacket. Combustion characteristics of the combustor were first analyzed based on 2D computational Fluid Dynamics (CFD), and then thermo-mechanical analysis on the combustor was carried out by means of 3D Finite Element Analysis (FEA) method. The results showed that the most dangerous locations where the critical failure could possibly occur lay at the burning areas in the recirculation jacket due to the poor bonding, the high temperature and the residual stress. The results of this study can be used for the design and improvement of the micro-combustors.

List of symbols

C_p	Specific heat (J/kg K)
EX	Elastic modulus (Pa)
K	Conductivity (W/m K)
T	Ambient temperature (K)
μ	Poisson's ratio
ρ	Density (kg/m^3)
σ_s	Yield strength (MPa)
h	Heat transfer coefficient on the outer wall (W/m^2 K)
V	Mass flow rate of the mixture (g/s)
ε	Radiation emissivity of silicon
δ	Equivalence ratios of the hydrogen/air mixture
α	Coefficient of thermal expansion of silicon

L. Zhu (✉) · C.-L. Yin · M. Zhu
School of Engineering, Anhui Agricultural University, Hefei 230036, People's Republic of China
e-mail: Zl009@mail.ustc.edu.cn

L. Zhu · T.-C. Jen · Y.-F. Ji
Mechanical Engineering Department, University of Wisconsin, Milwaukee, WI 53211, USA

1 Introduction

With the rapid development of various kinds of miniature devices such as notebook computers, mobile phones, medical devices, and walking robots etc., the availability of compact, highly mobile and efficient micro-power supply systems is becoming increasingly important in our daily lives. Currently, most of these devices are powered by batteries. They can only continuously work for certain period of time so that they may need recharging frequently (Mehra 2000; Hua et al. 2005a; Epstein 2003; Spadaccini 2004; Chen 1999). Therefore, developing a continuous, light weight, high power density and efficient micro-power source is great demanded to improve our quality of life. A combustion-based micro-gas turbine engine is one of the most promising micro-power sources because it has higher power density, smaller volume and less pollution than any other type of micro-power sources, e.g., micro fuel cells, etc. (Hua et al. 2005a).

The MIT group proposed the concept design of a micro-gas turbine engine and also has studied the combustion behavior in a stand-alone micro-combustor without the rotating parts of the micro-compressor and micro-turbine using the numerical and experimental methods. The results show that (Epstein 2003) the combustion could occur within the combustion chamber under certain designed

operating conditions in the laboratory. However, under more realistic application conditions, the performance of the micro-combustor may be affected by factors such as loading variation, environmental condition changes, etc. It has been observed (Hua et al. 2005a; Epstein 2003; Spadaccini 2004) in both experiments and numerical simulations that the flame burns in the recirculation jacket of the micro-gas turbine engine under the high equivalence ratio of the hydrogen/air mixture. Consequently, the combustor wall temperature could be higher than the upper limit of the material's allowable temperature, resulting in a short lifetime of the combustor. It is well known that the micro-combustor from MIT is made of silicon, and that the adiabatic flame temperature of premixed stoichiometric hydrogen/air mixture can reach as high as 2,400 K (Epstein 2003). Sufficient high temperature causes the yield strength of silicon to drop off rapidly, causing the transitions from a brittle to a plastic material and subsequent creep failure when the temperature is above 900 K (Chen 1999; Miki and Zhang 2003; Mehra et al. 1999; Park and Choi 2005; Chen et al. 2002). Therefore, it is very imperative to investigate the effects of the equivalence ratio of the hydrogen/air mixture on the structure of micro-combustor device. And furthermore, very few literatures have currently reported on effects of the different operation conditions on the structure of the micro-combustor device.

In this study, the influences of the equivalence ratio of the hydrogen/air mixture on the structure of the micro-combustor are investigated when its mass flow rate is constant. The most dangerous locations where the critical failure could possibly occur are predicted using a numerical simulation based on explicit CFD and FEA software.

2 CFD model and simulation approach

2.1 Model geometry

The micro-gas turbine engine proposed by the MIT group was fabricated using MEMS technology. It is composed of six wafers. Based on the geometries in Mehra (2000), Hua et al. (2005a), a 2D model of the micro-combustor in this study was constructed in Gambit using Frame Modeling Method. The combustor involved the important static components of the micro-gas turbine engine, including the recirculation jacket, flame holder, combustion chamber and stators of compressor and turbine. Since the combustion characteristics of the micro-combustor are the primary objective of this study, the effects of the rotating parts of compressor and turbine as well as the fuel injector in this model are not considered in this study. A schematic of the 2D micro-combustor model structure is illustrated in Fig. 1.

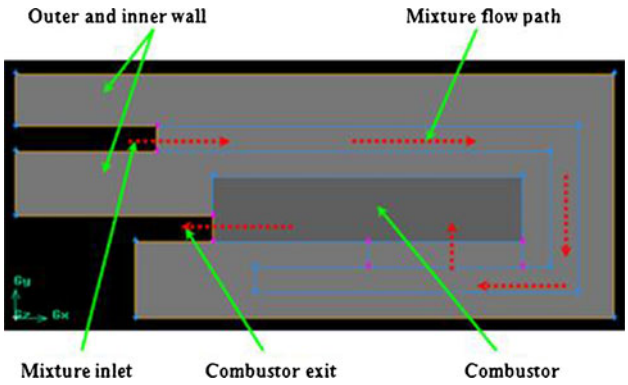

Fig. 1 Schematic of half of the axisymmetric 6-wafer silicon micro-combustor

As seen in Fig. 1, the hydrogen/air mixture is injected through the combustor inlet to the top recirculation jacket and mixes with each other as it flows through the recirculation jacket, enters the combustion chamber through a set of inlet ports along the combustor's axial direction, reacts in the annular combustion chamber, and finally exhausts through the outlet.

Figure 2 shows the meshed CFD model of the micro-combustor. The CFD model comprises of the hydrogen/air flow path, combustion chamber, as well as the conjugated heat transfer model in solid engine walls. Fluent 6.0 was used to perform the numerical analyses on fluid flow, heat transfer and the chemical reactions in the micro-combustor.

Distinguished from Hua et al. (2005a), CHEMKIN models in Fluent 6.0 were utilized to express the detailed chemical kinetics of hydrogen/air combustion. The detailed gas phase mechanism involved 19 reversible reactions and 9 species similar to those used in Hua et al. (2005a). A double precision, segregated solution solver was used to solve the governing equations.

The boundary conditions for the CFD modeling were defined to match the experimental conditions reported in Mehra (2000) as closely as possible. Symmetric boundary conditions were used for the two radial section models. Since the details of the compressor were neglectable in this model due to the lack of the required data, uniformly distributed temperature and velocity were assumed at the combustor inlet. For all the simulation cases in this paper, the inlet temperature of hydrogen/air was assumed to be 300 K, a fixed pressure of 1.01325×10^5 Pa was specified at the combustion chamber outlet, no-slip boundary conditions and no species flux normal to the wall surface were applied at the wall. The convective and radiative heat losses to the ambient at the external wall were also considered. For simplicity, constant convective heat transfer coefficient and radiative emissivity were assumed at the outer walls. In addition, the thermal conductivity of the

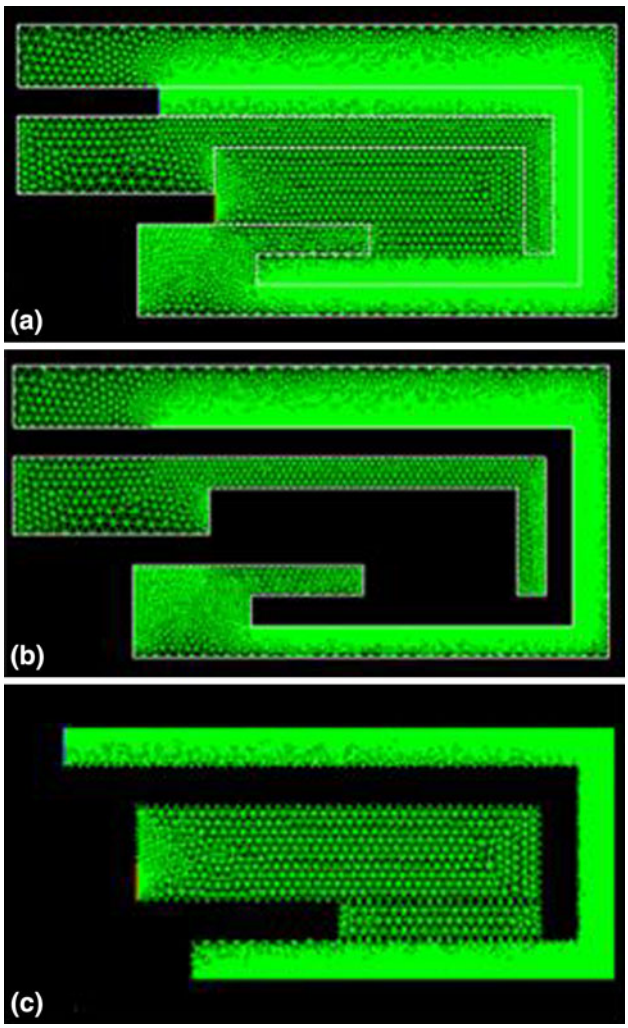

Fig. 2 **a** Total CFD mesh, **b** CFD mesh for heat exchange area, and **c** CFD mesh for flow and combustion area

micro-combustor wall was assumed to have a constant value at 149 W/(m K) for all the simulations in this paper.

2.2 Results and discussions

Because size of micro-combustion chamber is decreased to millimeter level, the surface area to volume ratio in micro-combustors becomes rather high, (0.500 m^{-1}), which is two orders of magnitude larger than that of a typical combustor (Epstein 2003). Energy loss due to heat transfer at the walls of the micro-combustor must not be neglected, because the heat loss through the wall plays a critical role in stabilizing the combustion in the micro-chambers. The high thermal conductivity of silicon and small length scales produce low heat resistance of the wall, which enhances the effect of heat loss through the outer wall (Epstein 2003).

In order to study the effect of the different equivalence ratios of the hydrogen/air mixture on the combustion in the micro-combustor, 2D Computational Fluid Dynamics (CFD) simulation was used here. And also, for the purpose of comparing the calculated results in the paper with Mehra (2000), the corresponding parameters were chosen as follows:

- $\delta = 0.4, 0.5, 0.6, 0.7$, respectively;
- $h = 200$ W/(m^2 K); $\varepsilon = 0.85$; $T = 300$ K; $V = 0.1$ g/s.

The velocity distribution of the mixture, when the equivalence ratio is 0.5, is shown in Fig. 3. The temperature distributions of the micro-combustor under the different equivalence ratios (a) 0.4, (b) 0.5, (c) 0.6, (d) 0.7 are presented in Fig. 4, respectively. In addition, in order to compare the numerical simulation results in this study with Mehra (2000), the corresponding experimental results are also illustrated in Figs. 5 and 6.

It can be seen from Fig. 3 that the velocity of the hydrogen/air mixture is diminishing when it enters the chamber. This may be due to the facts as follows:

- When the flow entering larger compartment of the combustion chamber, its velocity is accelerated at the bottom of the chamber, and furthermore, the high pressure due to the combustion in the chamber is generated. The combined effects of the larger velocity and the higher pressure can create a strong jet type of flow to hit the inner walls of the combustor and circulate through the chamber.
- The mixture has performed dozens of steps of reversible elemental chemical reactions in the combustion chamber, producing many interim resultants, so that their molecules collide with each other more frequently per unit time due to the micro-burning area.

Figure 4a–d illustrate the temperature distributions on the cross section of the micro-combustor with the equivalence ratios 0.4, 0.5, 0.6, and 0.7, respectively.

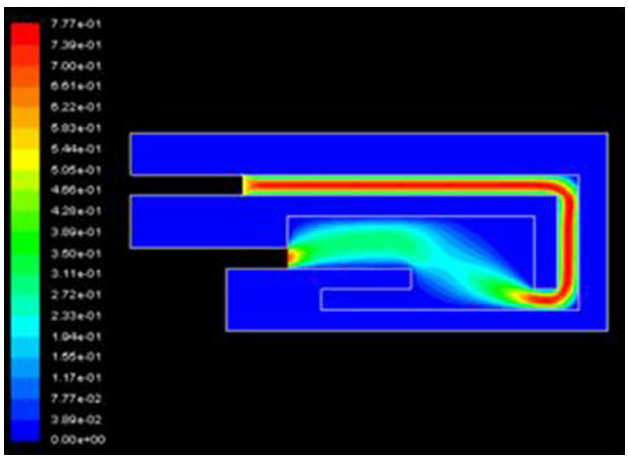

Fig. 3 Velocity distribution of the mixture with equivalence ratio 0.5

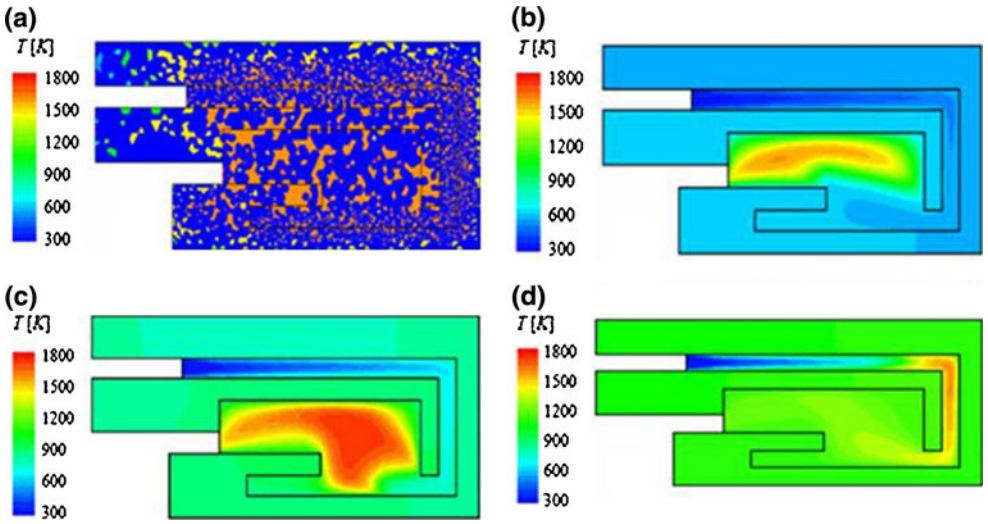

Fig. 4 Temperature distribution on the micro-combustor with different equivalence ratios of hydrogen/air mixture: **a** 0.4, **b** 0.5, **c** 0.6, **d** 0.7

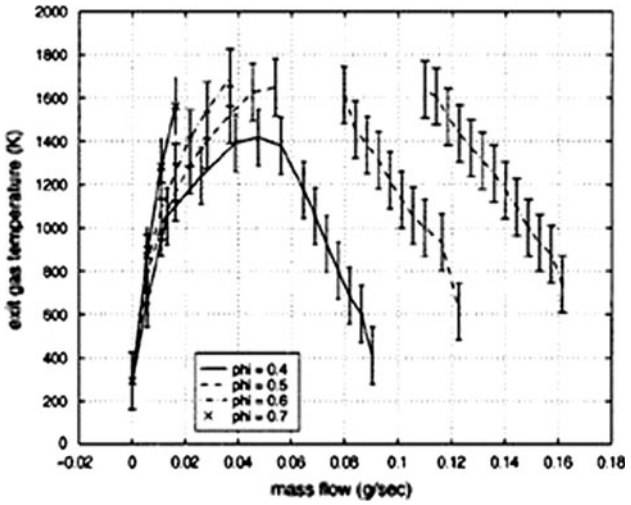

Fig. 5 Exit temperature measurements in the static structure as a function of mass flow rate for different fuel–air equivalence ratios (Mehra 2000)

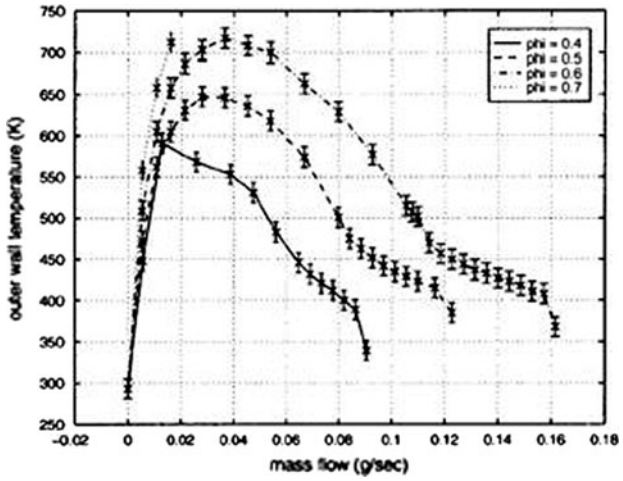

Fig. 6 Outer wall temperature measurements in the static structure as a function of mass flow rate for different fuel–air equivalence ratios (Mehra 2000)

As seen from Fig. 4b and c, it could draw a conclusion that the combustion could stabilize in the micro-chambers, and that both the exit gas temperature and the outer wall temperature increase correspondingly with increasing the equivalence ratio of the hydrogen/air mixture, which are in agreement with the experimental results in Figs. 5 and 6. This attributes to the fact that the flame speed is higher in the fuel/air mixture with higher equivalence ratio (less than 1). As the equivalence ratio is increased, a greater fraction of the combustion heat is contributed to heat up the gas phase to maintain the combustion. And then, the exit gas temperature and combustor efficiency increases, and the combustion will be more stable in the combustion chamber.

However, in Fig. 4a, it is observed that the flame in the combustion chamber could not sustain and even quench when the equivalence ratio of the mixture is set to be 0.4. This attributes to the facts that, on the one hand, the lower equivalence ratio of the mixture can result in the lower flame speed, subsequent causing the lower heat generation rate. On the other hand, the high surface area to volume ratio of the micro-combustor can induce significant heat loss from the outer wall of the micro-combustor. Consequently, the flammability of the hydrogen/air mixture gradually becomes less and less, and then the quenching phenomenon eventually occurs in the chamber.

It is worth paying special attention to Fig. 4d, where the upstream burning was observed. This also agrees with the experimental results in Mehra (2000). Due to the high thermal conductivity of silicon, the heat transfer through the outside wall plays a critical role in heat removal from

the micro combustor. When the equivalence ratio of the mixture is too high, as in this case (0.7), significantly great fraction of the combustion heat is contributed to heat up the gas phase, thus causing the exit gas temperature to become higher than before. And furthermore, insufficient heat can be removed from the outside environment. This results in the temperature at the combustor wall to increase significantly. The cold incoming reactants could be heated up in the recirculation jacket, and may burn in upstream of the recirculation jacket if their temperatures exceed the mixture ignition temperature, e.g. 858 K. The combustion in the recirculation jacket not only compromises the insulating properties of the jacket, but also has the possibility to damage the device (Hua et al. 2005a; Epstein 2003; Spadaccini 2004; Chen 1999). It is reported in Chen (1999) that the fracture toughness of single crystal silicon is found to be temperature independent below the brittle to ductile transition temperature (BDTT), and that, if the temperature is higher than BDTT, the material behavior of silicon becomes increasingly nonlinearly elastic and then ductile. For example, its yield strength is reduced to less than 50 MPa as the temperature approaches 1,200 K (Chen 1999). Therefore, the operation of micro-combustor at high equivalence ratio should be avoided.

However, between Figs. 4 and 5, 6 there exist some minor differences, especially on the magnitudes of the exit gas temperatures and the outer wall temperatures. This is due mainly to the lack of the required data on some geometric dimensions and the appropriate boundary conditions. Owing to the insufficient data on the structure of the micro-combustor, some assumptions were made based on Hua et al. (2005a) when constructing the CFD model in this study. Therefore, we consider that these simplified assumptions and the inappropriate boundary conditions may have some effects on the final simulation results.

3 Structural analysis

In order to further investigate the behavior of the micro-combustor under various equivalence ratios when the mass flow rate of the hydrogen/air mixture is constant, it is very imperative to perform the structural analysis on the micro-combustor, especially when the equivalence ratio is sufficiently high. The micro-combustor is etched from single crystal silicon using MEMS fabrication technique. Presently, the fracture strength of silicon under the room temperature is reported to be extremely sensitive to the surface processing method (Chen 1999; Mehra et al. 1999; Park and Choi 2005; Chen et al. 2002; Klaasen et al. 1996) and there are several fabrication issues that have to be resolved before multilayered structures can be successfully built (Miki and Zhang 2003; Mehra et al. 1999). All of these have deleterious effects on the structural strength of the micro-combustor, and furthermore, the order of magnitude of thermal stresses can become as high as the available material yield strength if the structural temperature and temperature gradient are sufficiently high. Therefore, 3D finite Element Analysis Method based on commercial software COSMOS\works is utilized to investigate the thermo-mechanical problems on the structural design of the micro-combustor in this study.

3.1 Analysis on fabrication process of the micro-combustor

The fabrication of the combustor required ten deep dry anisotropic etches and two shallow etches, in which a total of 13 masks were necessitated, including one global alignment mask. The process consisted of deep reactive ion etching, photolithography and aligned fusion bonding (Mehra et al. 1999). Normally, during constructing the multi-layered structures there exist several bonding issues to resolve (Park and Choi 2005); they are (1) surface contamination issues, (2) stiffness related issues (increased stiffness), (3) bonding tool effects, and (4) defect propagation. Among them, items 1, 2 and 3 are considered to be more serious.

For 1, although it is possible to successfully bond several prime silicon wafers, the same task can be difficult to achieve with processed wafers because of the presence of residual films on which the surfaces to be bonded are contaminated (see Fig. 7).

For 2, multi-stack bonding becomes increasingly difficult when thick wafers or previously bonded stacks are used as a result of bow and warpage. The failing interface is located between wafer 3 and wafer 4 in the experiment because of the large stiffness.

For 3, the presence of particulates on surfaces to be bonded as well as the appearance of protrusions that locally

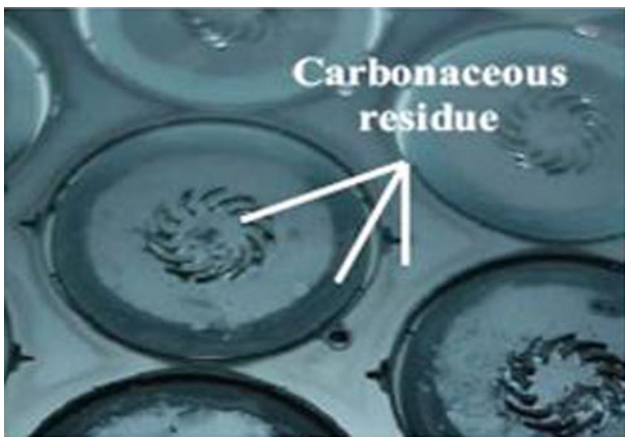

Fig. 7 Carbonaceous residue observed on some surface after DRIE (Miki and Zhang 2003)

distort a wafer surface can have a deleterious effect on yield or preclude additional bonds. A postmortem analysis indicated that the source of the defects was located at the interface between wafers 3 and 4, and the defects created protrusions on the surface of the fourth wafer that was to be bonded to the subsequent fifth wafer (see Fig. 8).

3.2 Analysis on the structure of the micro-combustor

As depicted above, when the equivalence ratio of the mixture increases to a certain value, the flame front could burn in the recirculation jacket, causing the wall temperature near the flame to be as high as 1,200 K. This may further aggravate the bow and warpage effect on the wafers, especially between wafer 3, 4 and 5. Before performing the structural analysis on the micro-combustor, three important assumptions are made to make the problem tractable (Chen et al. 2002; Hua et al. 2005b; Klaasen et al. 1996; Mehra et al. 1999; Mehra and Waitz 1998; Miki and Zhang 2003; Park and Choi 2005; Spadaccini et al. 2003). Some discussions about these assumptions are listed as follows:

- Neglect the high-temperature oxidation results of silicon

It has been validated that the "active-oxidation" of silicon is not an overriding concern for this particular application. A careful examination of the results obtained from the experiments indicated that the structure of the micro-combustor remained intact even after exposure to a combustion environment for over 8 h at atmospheric pressures and flow temperatures in excess of 2,000 K. Therefore, it is reasonable to neglect the high temperature oxidation results of silicon when performing the structural analysis on the micro-combustor.

- Ignore residual stress from the fabrication process of the micro combustor

Numerical simulation results have shown that thermal stress is more influential on fatigue life although its value is smaller than residual stress, and furthermore there exist insufficient data on the residual stress in the fabrication process. The effect of residual stresses is therefore inconclusive.

- Emphasize the creep result of silicon due to the high temperature above BDTT

Creep failure is believed to be the primary failure mode for silicon in high temperature micro-combustor environments.

Therefore, this study focuses on thermal stress and strain analysis on the structure at high temperatures.

As illustrate in Fig. 9, the creep failure may occur at the two locations of the micro-combustor when upstream burning occurs in the recirculation jacket. The first position may be located at the interface of wafers 1, 2 and 3 (see the red dashed ellipse), because there are sharp angles where the stress could be congregated enough to promote creep failure easily due to the impact of large periodic thermal power input. The other may be located at the interface of wafers 3 and 4. It is observed in the experiment that the defects were located at the interface between wafers 3 and 4 (see the black rectangle), and that they created protrusions on the surface of the fourth wafer that was to be bonded to the subsequent fifth wafer (see Fig. 8). Under the impact of the large periodic thermal power inputs, the protrusions on the wafer 4 could become larger than before, resulting in a poor bonding strength and the failure.

3.3 Finite element analysis on wafers 1, 2, and 3

Having thoroughly analyzed Fig. 9 and the fabrication processes of the micro-combustor, we considered that the failure location at the junction of wafers 1, 2, and 3 was actually at the bonded position between the tail of wafer 3 and wafers 1 and 2 (see the red arrowhead in Fig. 10). This can be explained as follows: bow and warpage may occur at this location due to stress concentration in the process of fabrication (Park and Choi 2005; Bagdahn et al. 2003), and moreover, the bow and warpage effects aforementioned may be further aggravated due to the significantly high temperatures, 1,700–1,800 K in the recirculation jacket and

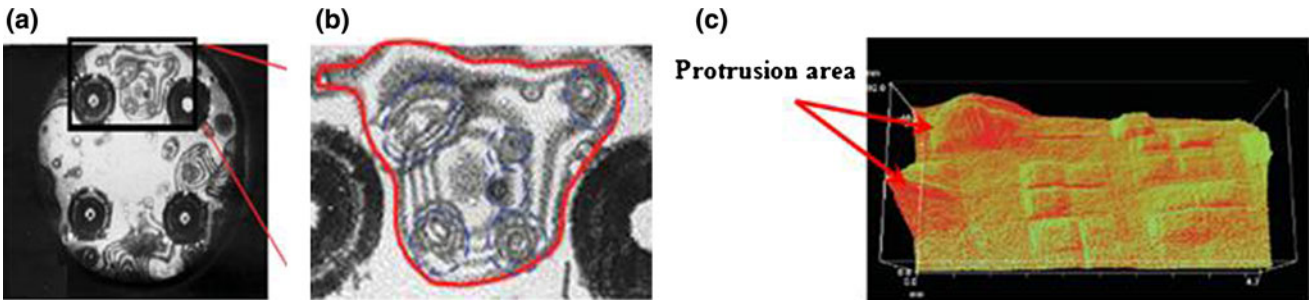

Fig. 8 **a** IR image of 5-wafer stack, **b** close-up view of a protrusion, and **c** surface image of the propagated defects (Miki and Zhang 2003)

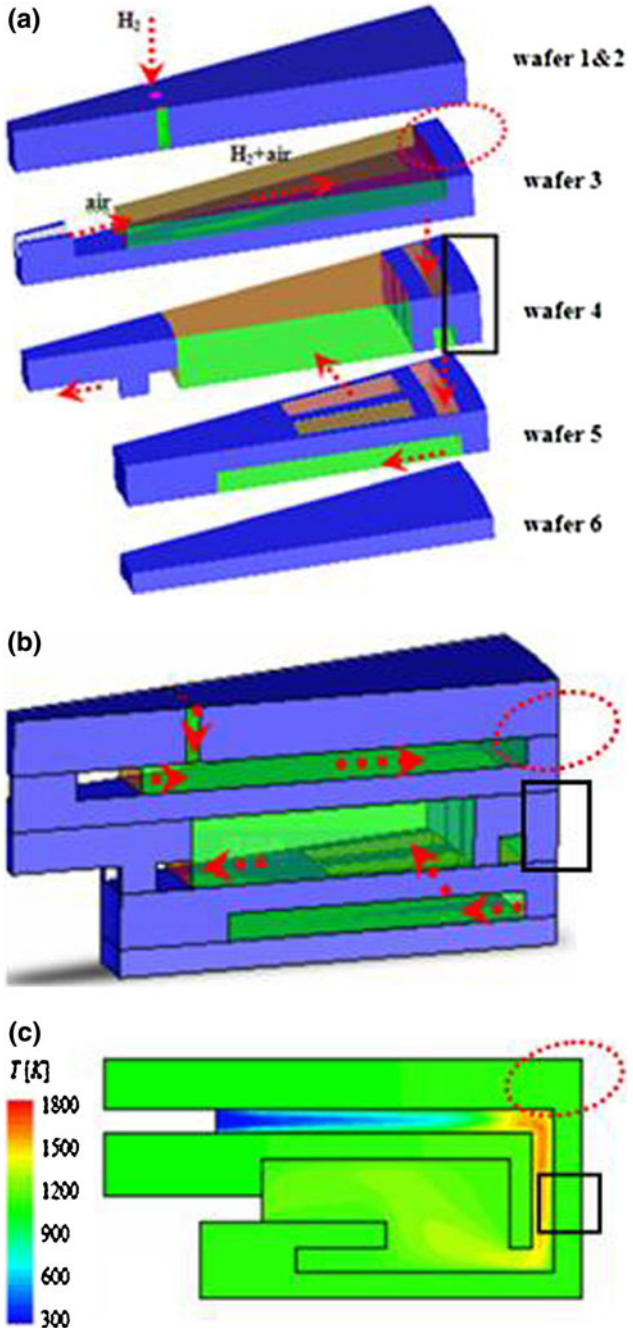

Fig. 9 Flow of the mixture in **a** an exploded view, **b** an unexploded view, and **c** temperature distribution on the micro-combustor with upstream burning in the recirculation jacket

1,000–1,200 K on the outer wall. Therefore, a FEM analysis was performed on the tail of wafer 3 (see (b) in Fig. 10), in which the green arrowhead indicated the flow direction of the mixture.

The grid convergence test showed grid size of 11,302 nodes and 6,526 elements yielded the reliable results. The material used here was single crystal silicon, whose physical properties are (Chen 1999):

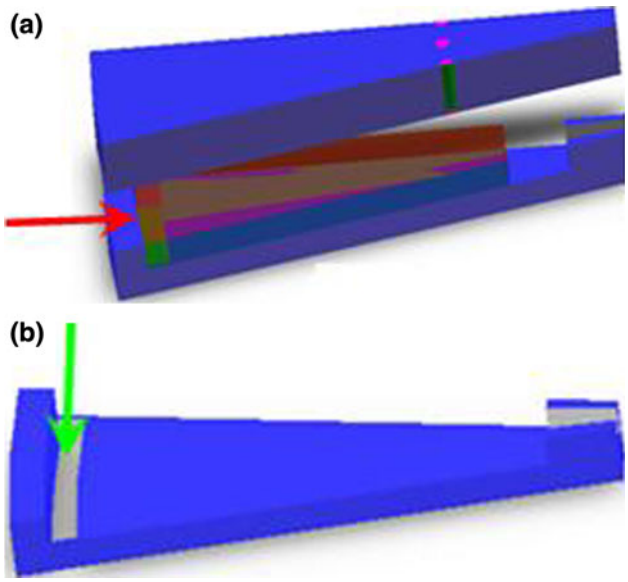

Fig. 10 **a** Schematic of wafers 1, 2, and 3, **b** wafer 3

- $EX = 1.69 \times 10^{11}$ Pa; $\mu = 0.28$; $\sigma_s = 50$ MPa; $\rho = 2{,}300$ kg/m^3;
- $C_p = 700$ J/(kg K); $K = 32$ W/(m K); $h = 300$ W/(m^2 K).

It can be seen from Fig. 11 that the peak stress occurs at the interface of wafers 1 and 2 and wafer 3, namely the bonded location of wafers 1 and 2 and wafer 3. The maximum stress is equal to be 30.38 MPa. Just at the same location there exists the maximum strain, which equals to 1.092×10^{-4} (see Fig. 12). The maximum thermal stress and strain may have a deleterious effect on the bonded location between wafers 1 and 2 and wafer 3. Consequently, under the combined effects of the congregated stress, the poor bonding, the highest thermal stress and strain, the failure may occur at the interface of wafers 1 and 2 and wafer 3 during the combustion processes in the micro-combustor.

3.4 Finite element analysis on wafers 3 and 4

Similarly, as a result of the poor bonding in the process of fabrication and the high temperature from the flame burning in the recirculation jacket, the failure location at the interface of wafers 3 and 4 is believed to lie at the bonded position between the tail of wafer 4 and wafers 1 and 2 and 3 (see the yellow arrowhead in Fig. 13). A FEM analysis is carried out on the tail of wafer 4 (see (c) in Fig. 13), where the red arrowhead indicates the flow direction of the mixture.

A total of 10,568 nodes and 6,401 elements were used in this case study after performing grid convergence test.

From Fig. 14, it can be seen that the peak stress occurs at the interface of wafers 3 and 4, namely the outer fringe

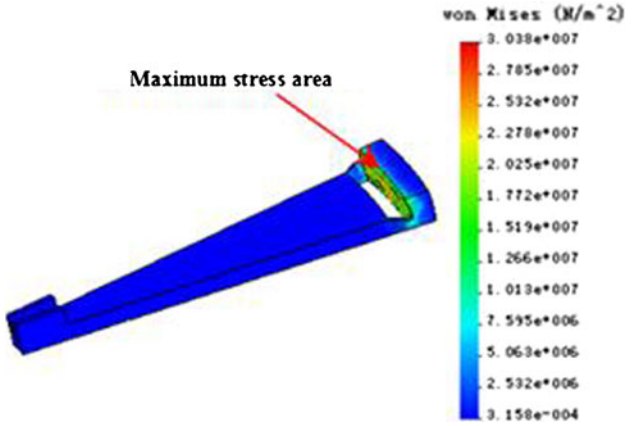

Fig. 11 Thermal stress distribution in the wafer 3

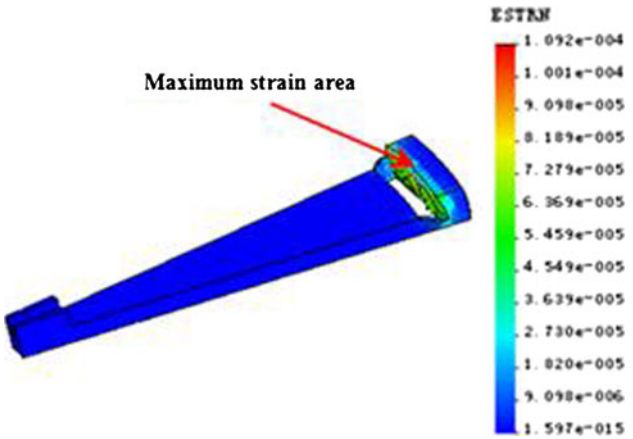

Fig. 12 Thermal strain distribution in the wafer 3

of the junction. The maximum stress is 29.98 MPa. Similarly, at the same location there also exists the maximum strain, which equals to 9.803×10^{-5} (see Fig. 15). The numerical simulation results reveal that the bow and warpage due to high temperature at the outer wall occurs at the bonded locations. Therefore, it is considered that the high thermal stress and strain may further aggravate the bow and warpage effects from the fabrication process, making the protrusions on the surface of the fourth wafer (see Fig. 8) become larger than before. Consequently, this may significantly decrease the bonding strength in the fifth wafer, and result in the combustion chamber failure.

In order to further verify the deleterious effect resulting from wafers 1 and 2 and wafer 3 as well as wafers 4 and 5 during the combustion processes, the interfaces of the other wafers in the combustor, e.g. the interface between wafer 3 and 4, the interface between 5 and 6, were also calculated using the FEA method. The results are illustrated in Fig. 16, where distance denotes the length measured from the inner wall toward the outer wall (see the yellow arrowhead in Fig. 13). The depth simulated is up to 0.5 mm.

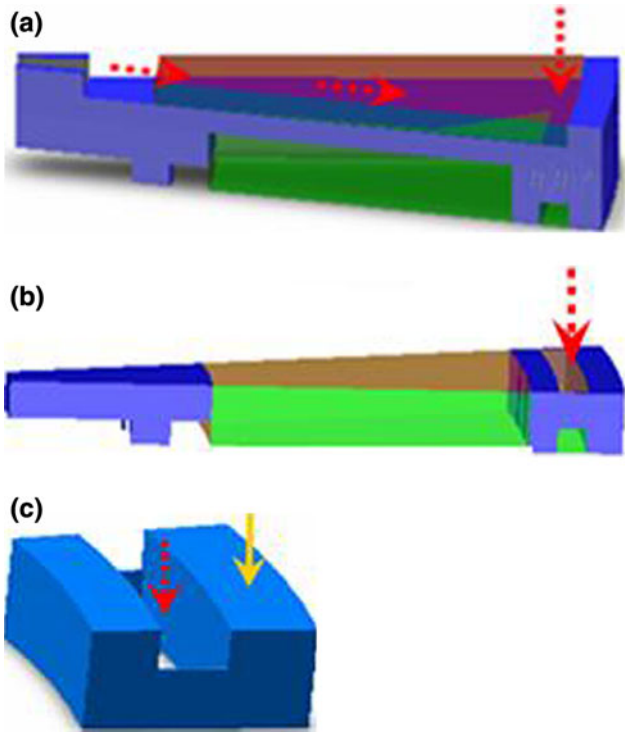

Fig. 13 **a** Schematic of wafers 3 and 4, **b** wafer 4, and **c** the tail of wafer 4

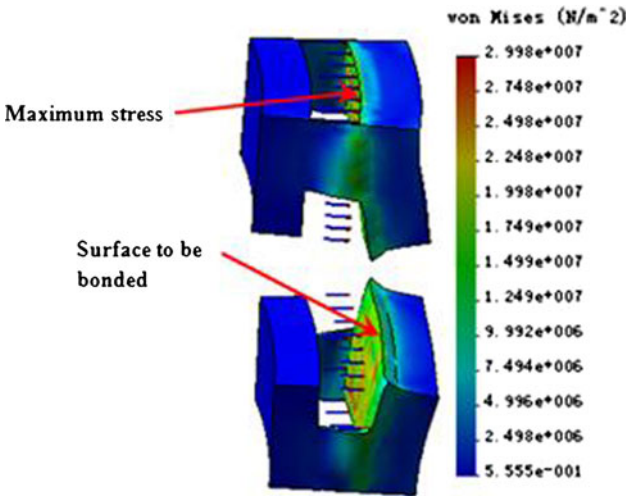

Fig. 14 Thermal stress distribution on the tail of wafer

From Fig. 16, it could be inferred that the thermal stresses on either wafers 1, 2, and 3 or wafers 4 and 5 are much higher than those on wafers 3 and 4 and wafers 5 and 6, and that the thermal stresses become less and less with approaching closer to the fringe of the outer wall.

Although the thermal stresses (30.38 and 29.98 MPa) calculated in this study are small for lower temperature, at the current level of temperature (>1,200 K), they are comparable to the available strength (~50 MPa), and

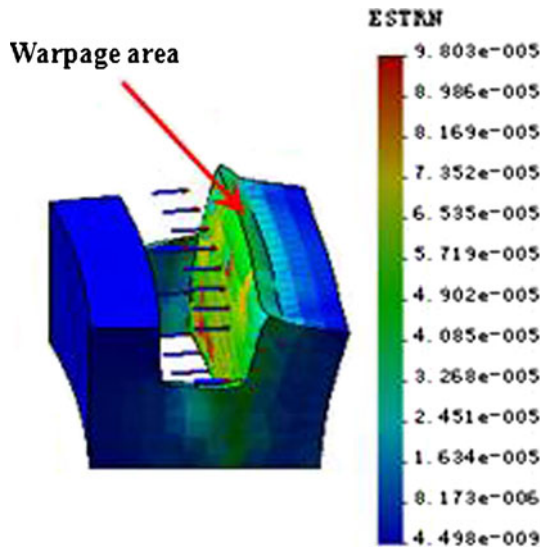

Fig. 15 Thermal strain distribution on the tail of wafer 4

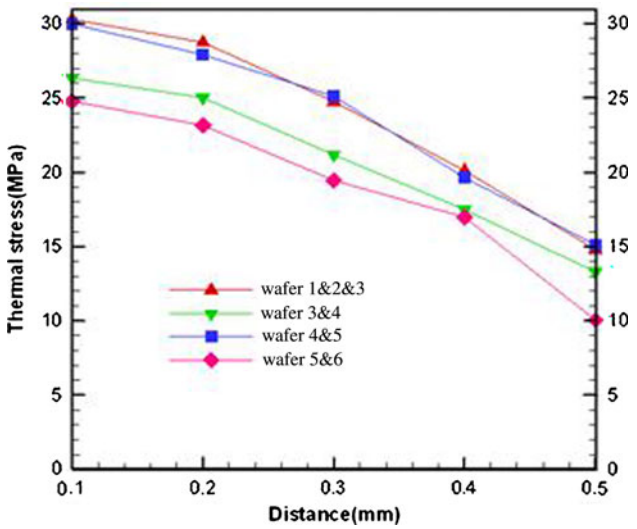

Fig. 16 Comparative thermal stress distribution on the different interfaces of wafers

furthermore, the order of magnitude of such thermal stresses can be as high as the available material yield strength if both the structural temperature and temperature gradient are sufficiently high. Additionally, the residual stresses in the fabrication process of the micro-combustor are negligible due to the insufficient data related, but they may have deleterious effects on the micro-combustor (Zhang et al. 2000; Zhang and Chen 2002). Therefore, under the combined impacts of the congregated stress, the poor bonding, the high thermal stress and the residual stresses, the bonding junctions of wafers 1, 2, and 3 as well as wafers 4 and 5 could be weakened so much that fatigue failure may occur.

4 Conclusion

Under the different equivalence ratios of the hydrogen/air mixture, the 2D CFD based numerical simulation results indicate that the flame could be sustained in the micro-combustor if the equivalence ratio of the mixture is most suitable. However, the combustor wall temperature could be higher than the auto ignition temperature of reactants if the equivalence ratio increases to a certain value. The numerical simulation results in this study are in excellent agreement with those in the corresponding experimental evidence. Since sufficiently high temperature of the outer wall possibly damages the device due to the upstream burning, optimizing the equivalence ratio of the hydrogen/air mixture is a most effective approach to manage the combustor wall temperature.

For a silicon six-wafer micro-combustor, the thermal stress may be a significant design restriction in the stationary structure due to the higher temperature (and lower strength). Thus, thermo-mechanical analysis on static structure is required to provide the information on the overall micro-combustor engine redesign.

Based on the CFD simulated temperature distribution on the micro-combustor, 3D FEM method is utilized to investigate the effect of the equivalence ratio of the hydrogen/air mixture on the structure of the micro-combustor device. The results indicate that the thermal stress due to sufficiently high temperature may further weaken the strength of bonding and accelerate the failure of the combustor. The results from this study can be used to define geometric parameters for optimal design of the micro-combustor.

Acknowledgments Dr. Lin Zhu would like to thank the financial support for the project from the Chinese National Foundation (50721140651), Anhui Province National Foundation (KJ2009B004Z), and Anhui Agricultural University Applied Research Grant (wd2008-6). Dr. Tien-Chien Jen would also like to acknowledge the partial financial support from EPA (RD833357) and Research Growth Initiative II from University of Wisconsin, Milwaukee.

References

Bagdahn J, Sharpe WN Jr (2003) Fracture strength of polysilicon at stress concentrations. IEEE J Microelectromech Syst 12:302–312

Chen KS (1999) Materials characterization and structural design of ceramic micro turbomachinery. Ph.D. thesis, Massachusetts Institute of Technology, Cambridge, MA

Chen KS, Ayon AA, Zhang X (2002) Effect of process parameters on the surface morphology and mechanical performance of silicon structures after deep reactive ion etching. IEEE J Microelectromech Syst 11:264–275

Epstein AH (2003) Millimeter-scale, MEMS gas turbine engines. In: Proceedings of ASME Turbo Expo 2003 Power for Land, Sea, and Air (2003), vol 6, pp 16–19

Hua J, Wu M, Kumar K (2005a) Numerical simulation of the combustion of hydrogen–air mixture in micro-scaled chambers

Part II: CFD analysis for a micro-combustor. Chem Eng Sci 60:3507–3515

Hua J, Wu M, Kumar K (2005b) Numerical simulation of the combustion of hydrogen–air mixture in micro-scaled chambers Part I: fundamental study. Chem Eng Sci 60:3497–3506

Klaasen EH, Petersen K, Noworolskil JM (1996) Silicon fusion bonding and deep reactive ion etching: a new technology for microstructures. Sens Actuators A 52:132–139

Mehra A (2000) Development of a high power density combustion system for a silicon micro gas turbine engine, Ph.D. thesis, Massachusetts Institute of Technology, Cambridge, MA

Mehra A, Waitz IA (1998) Development of a hydrogen combustor for a microfabricated gas turbine engine. In: Solid state sensor and actuator workshop 1998, pp 224–231

Mehra A, Ayón AA, Waitz IA, Schmidt MA (1999) Microfabrication of high temperature silicon devices using wafer bonding and deep reactive ion etching. IEEE J Microelectromech Syst 8:152–160

Miki N, Zhang X (2003) Multi-stack silicon-direct wafer bonding for 3D MEMS manufacturing. Sens Actuators A 103:194–201

Park JH, Choi HC (2005) FEM analysis of multilayered MEMS device under thermal and residual stress. J Microsyst Technol 11:925–933

Spadaccini CM (2004) Combustion systems for power-MEMS applications. Ph.D. thesis, Massachusetts Institute of Technology, Cambridge, MA

Spadaccini CM, Jin L, Zhang X (2003) High power density silicon combustion system for micro gas turbine engines. J Eng Gas Turbines Power 125:709–719

Zhang X, Chen KS (2002) Residual stress and fracture of thick dielectric films for power MEMS applications. IEEE J Microelectromech Syst 11:164–167

Zhang X, Ghodssi R, Chen KS (2000) Residual stress characterization of thick PECVD TEOS film for power MEMS applications. In: Solid state sensor and actuator workshop 2000, pp 316–319